

---

This is the **accepted version** of the article:

Chen, Wei Wei; Takahashi, Nozomu; Hirata, Yoshito; [et al.]. «A mobile ELF4 delivers circadian temperature information from shoots to roots». Nature plants, Vol. 6, issue 4 (April 2020), p. 416–426. DOI 10.1038/s41477-020-0634-2

---

This version is available at <https://ddd.uab.cat/record/221269>

under the terms of the  **IN COPYRIGHT** license

**A mobile ELF4 delivers circadian temperature information from shoots to roots**

Wei Wei Chen<sup>1\*</sup>, Nozomu Takahashi<sup>1\*</sup>, Yoshito Hirata<sup>2,3</sup>, James Ronald<sup>4</sup>, Silvana Porco<sup>5</sup>, Seth J. Davis<sup>4,6</sup>, Dmitri A. Nusinow<sup>7</sup>, Steve A. Kay<sup>5,8</sup> and Paloma Mas<sup>1,9,†</sup>.

<sup>1</sup>Centre for Research in Agricultural Genomics (CRAG), CSIC-IRTA-UAB-UB, Campus UAB, Bellaterra, 08193 Barcelona, Spain.

<sup>2</sup>Mathematics and Informatics Center, The University of Tokyo, 7-3-1 Hongo, Bunkyo-ku, Tokyo 113-8656, Japan.

<sup>3</sup>Faculty of Engineering, Information and Systems, University of Tsukuba, 1-1-1 Tennodai, Tsukuba, Ibaraki 305-8573, Japan.

<sup>4</sup>Department of Biology, University of York, York, UK.

<sup>5</sup>Keck School of Medicine, University of Southern California, Los Angeles, California 90089, United States.

<sup>6</sup>Key Laboratory of Plant Stress Biology, School of Life Sciences, Henan University, Kaifeng 475004, China.

<sup>7</sup>Donald Danforth Plant Science Center, St. Louis, MO 63132.

<sup>8</sup>Institute of Transformative Bio-Molecules, Nagoya University, Nagoya 464-8601, Japan.

<sup>9</sup>Consejo Superior de Investigaciones Científicas (CSIC), 08028 Barcelona, Spain.

\*These authors contributed equally the manuscript.

†Correspondence to: [paloma.mas@cragenomica.es](mailto:paloma.mas@cragenomica.es)

30     **Abstract**

31     The circadian clock is synchronized by environmental cues, mostly by light and temperature.  
32     Elucidating how the plant circadian clock responds to temperature oscillations is crucial to  
33     understand plant responsiveness to the environment. Here we found a prevalent temperature-  
34     dependent function of the Arabidopsis clock component ELF4 (EARLY FLOWERING 4) in the  
35     root clock. Although the root clock is able to run in the absence of shoots, micrografting assays  
36     and mathematical analyses show that ELF4 moves from shoots to regulate rhythms in roots.  
37     ELF4 movement does not convey photoperiodic information but trafficking is essential to  
38     control the period of the root clock in a temperature-dependent manner. At low temperatures,  
39     ELF4 mobility is favored, resulting in a slow-paced root clock while high temperatures decrease  
40     movement, leading to a faster clock. Hence, the mobile ELF4 delivers temperature information  
41     and establishes a shoot-to-root dialogue that sets the pace of the clock in roots.

42

43

44     **Introduction**

45     Nearly all photosensitive organisms have evolved timing mechanisms or circadian clocks able  
46     to synchronize metabolism, physiology and development in anticipation to the 24-hour  
47     light/dark cycles<sup>1</sup>. In *Arabidopsis thaliana*, the molecular clockwork is based on complex  
48     regulatory networks of core clock components that generate rhythms in a myriad of biological  
49     outputs<sup>2, 3</sup>. Appropriate phasing of biological processes relies on clock resetting by light and  
50     temperature cues; a mechanism that requires effective changes in the expression and activity of  
51     essential clock components<sup>4</sup>. Circadian clocks are also defined by a conserved feature known as  
52     temperature compensation<sup>5</sup>. In contrast to the temperature dependency of many  
53     physicochemical and biological activities, the circadian clock is able to maintain a constant  
54     period over a range of physiological temperatures. By virtue of different transcriptional, post-  
55     transcriptional and post-translational mechanisms<sup>6-9</sup>, the plant circadian system buffers the  
56     circadian period length. Therefore, the circadian clock is able to sustain a period close to 24-  
57     hours within a physiological range of temperatures. An ample collection of light-related  
58     factors<sup>10-14</sup> and clock-associated components<sup>9, 15, 16</sup> has been shown to directly or indirectly  
59     regulate clock temperature compensation in plants.

60

61     Among the Arabidopsis clock components, ELF4 (EARLY FLOWERING 4) was initially  
62     identified by its role in photoperiod perception and circadian regulation<sup>17</sup>. Structural and  
63     functional studies provided a view of the multiple entry points of ELF4 function within the  
64     clock<sup>18</sup>. ELF4 protein assembles into a tripartite complex (Evening Complex, EC) together with  
65     ELF3 and LUX ARRHYTHMO or PHYTOCLOCK1 (LUX/PCL1)<sup>19, 20</sup>. The complex regulates

growth and represses circadian gene expression<sup>21,22</sup>. ELF4 promotes the nuclear localization of ELF3<sup>19</sup> while LUX directly binds to the promoters of the target genes and thus facilitates the recruitment of ELF4 and ELF3<sup>20,23</sup>. Loss-of-function mutants of any of the EC components lead to arrhythmia<sup>17,24-26</sup>. Through multiple interactions with light, clock and photomorphogenesis related factors<sup>27</sup>, the EC is able to coordinate plant responses to environmental cues including temperature<sup>15,27-31</sup> although ELF4, ELF3 and LUX also display independent functions from the EC<sup>31-33</sup>.

Regarding the circadian structure and organization within the plant, it is broadly accepted that every plant cell harbors a circadian oscillator. However, circadian communication or coupling among cells and tissues varies at different parts of the plant<sup>34-38</sup>. For instance, while cotyledon cells present circadian autonomy<sup>39</sup>, different degrees of cell-to-cell coupling have been reported in leaves<sup>40-42</sup>, in the vasculature with neighbor mesophyll cells<sup>43</sup>, in guard cells<sup>44</sup>, in cells at the root tip<sup>45,46</sup> and within the shoot apex<sup>47</sup>. Long-distance shoot-to-root photosynthetic signaling is also important for clock entrainment in roots<sup>48</sup> and light piping down the root<sup>49</sup> contributes to this entrainment. Micrografting assays and shoot excision<sup>47</sup> suggest the existence of a long-distance mobile circadian signal from shoots to roots. Here we report that ELF4 moves from shoots to control the pace of the root clock in a temperature-dependent manner.

## Results

### Prevalent function of ELF4 sustaining rhythms in roots

We first approached the investigation of the circadian mobile signal by simultaneously following rhythms in shoots and roots of intact plants<sup>47</sup>. The waveforms of the morning-expressed *CCA1* (*CIRCADIAN CLOCK ASSOCIATED 1*) and *LHY* (*LATE ELONGATED HYPOCOTYL*) promoter activities displayed a long period, slightly reduced amplitude and phase delay in roots (Rt) compared to shoots (Sh) (Fig. 1a-b and Extended Data Fig. 1a). The mRNA rhythmic accumulation assayed by Reverse Transcription-Quantitative Polymerase Chain Reaction (RT-QPCR) followed the same trend (Fig. 1c). Similar patterns were observed for the promoter activity of the evening-expressed clock component *TOC1/PRR1* (*TIMING OF CAB EXPRESSION1/PSEUDO RESPONSE REGULATOR1*) (Extended Data Fig. 1b-c). Therefore, the clock is fully operative in roots but its overall pace is slower and the phase delayed compared to shoots.

Under free-running conditions, the circadian clock is unable to properly run in mutant plants of any of the EC components<sup>17,24-26</sup>. We therefore examined the role of the EC components in the root clock, and in particular, we focused on ELF4. Circadian time course analyses showed that although some very weak oscillations could be appreciated (Extended Data Fig. 1d), the *CCA1*

and *LHY* promoter activities and mRNA expression was suppressed in *elf4-1* mutant compared to WT roots (Fig. 1d and Extended Data Fig. 1e-g) following a similar trend to that described in shoots<sup>22</sup> (Extended Data Fig. 1h-j). Over-expression of ELF4 (ELF4-ox) lengthened the period of *LHY::LUC* (Fig. 1e and Extended Data Fig. 1k) indicating that increased ELF4 activity in roots makes the clock to run slow. The expression of *PRR9* (*PSEUDO-RESPONSE REGULATOR 9*), a previously described direct target of the EC in shoots, was clearly up-regulated in *elf4-1* mutant roots (Fig. 1f) suggesting that the EC also represses *PRR9* in roots. Thus, ELF4 plays an important regulatory function in the root clock: mutation compromises rhythms while over-expression lengthens the circadian period.

RNA-Seq analyses of WT and *elf4-1* mutant roots provided a genome-wide view of ELF4 function in roots (Supplementary Table 1). We found that about 15% of the root genes were significantly mis-regulated by the absence of a functional ELF4, with a similar proportion of up-regulated (1297) and down-regulated (1555) genes (Fig. 1g-h and Extended Data Fig. 2a). The expression of core clock genes was amongst the most significantly mis-regulated (Fig. 1i, Extended Data Fig. 2b-i) with a significant fraction of the mis-regulated genes being controlled by the clock, with phase enrichments during the subjective morning and subjective midday (Fig. 1j-k). Functional analyses showed that in addition to the enrichment of genes related to the circadian system and rhythmic processes, genes mis-expressed in *elf4-1* mutant were ascribed to several functional categories including among others responses to stimuli (Supplementary Table 1). Consistently, mis-expression of ELF4 affected physiological outputs such as the number of lateral roots (Extended Data Fig. 2j). Together, the results indicate a prevalent function for ELF4 sustaining rhythms in roots.

#### **ELF4 moves from shoots to regulate oscillator gene expression in roots**

Our previous study showed that a signal from shoots is important for circadian rhythms in roots<sup>47</sup>. Micrografting assays are a powerful tool to identify the nature of mobile signals. The grafting technique *per se* does not alter the rhythms in roots<sup>47</sup>, as grafted WT scions into WT roots show similar rhythms as non-grafted WT plants (Extended Data Fig. 3a and b). By micrografting different genotypes, we found that grafts of ELF4-ox shoots into *elf4-1* rootstocks [ELF4-ox(Sh)/*elf4-1*(Rt)] (Extended Data Fig. 3c) were particularly efficient in recovering the rhythms in roots (Fig. 2a and Extended Data Fig. 3d). The results are noteworthy as *CCA1::LUC* rhythms are affected in *elf4-1* mutant roots (Fig. 1d). Restoration of the rhythms was reflecting the circadian function exclusively in roots as water instead of luciferin was applied to shoots (ELF4-ox, Sh, H<sub>2</sub>O) to avoid luminescence signals leaking from shoots into roots of adjacent wells. Rhythms in roots were also recovered when ELF4-ox scion was grafted into *elf4-2* mutant (Extended Data Fig. 3e) rootstocks (Fig. 2b). To exclude the possibility that the

140 observed results were due to the high over-expression of ELF4-ox plants, we grafted WT shoots  
141 into *elf4-1* roots. Although the recovery of the rhythms was not as robust as with ELF4-ox  
142 grafts, a rhythmic pattern was observed in roots (Fig. 2c). Thus, ELF4 mRNA or protein are  
143 able to move from shoots to roots. This notion was reinforced by the results showing the  
144 rhythmic recovery of *elf4-1* rootstocks grafted with ELF4 Minigene (E4MG) scion (Fig. 2d and  
145 Extended Data Fig. 3f). These results rule out the possibility that the recovery of the rhythms  
146 was just due to the high over-expression of ELF4-ox scion. The influence of shoots as a driving  
147 rhythmic force of *elf4-1* rootstocks was also mathematically analyzed with recurrence plots  
148 obtained by delay coordinates of the grafting time series. The waveforms of the driving  
149 rhythmic force reconstructed from the driven system and their autocorrelation analyses showed  
150 a strong periodicity after grafting (Extended Data Fig. 4a-h). In analyses with 10000 randomly  
151 shuffled surrogates using as null hypothesis of no serial dependence, we obtained before  
152 grafting a p-value of 0.2341 (black dash line) (Extended Data Fig. 4f) and 0.0004 (gray dash  
153 line) after grafting (Extended Data Fig. 4h). The statistics are therefore consistent with the  
154 notion that rhythms in roots are being forced by a signal from shoots.

155

156 To investigate whether the mRNA could be the mobile signal, we performed RT-QPCR time  
157 course analyses of roots from ELF4-ox (Sh)/*elf4-1*(Rt) grafts. Our results showed no detectable  
158 amplification of *ELF4* mRNA at any time point analyzed (Fig. 2e), which suggest that *ELF4*  
159 mRNA did not move through the graft junctions. To confirm this notion, we injected purified  
160 ELF4 protein into *elf4-1* mutant (Extended Data Fig. 5a-c). Injection in shoots was able to  
161 restore rhythms in roots (Fig. 2f). The percentage of ELF4-injected plants with recovered  
162 rhythms was low (5-8%) but was reproducibly observed in different biological replicates. The  
163 fact that rhythms were actually restored (Relative Amplitude Errors, RAE<0.6) is supportive of  
164 a mobile ELF4 protein from shoots to roots. Rhythmic recovery was not apparent when purified  
165 GFP (GREEN FLUORESCENT PROTEIN) was injected (Fig. 2f). The movement of ELF4  
166 protein was further assayed by using shoots of plants over-expressing ELF4 fused to GFP  
167 grafted into *elf4-1* mutant roots. Confocal imaging showed that ELF4-GFP fluorescent signals  
168 accumulated in the vasculature of *elf4-1* mutant rootstock, across the graft junctions (Fig. 2g-h  
169 and Extended Data Fig. 5d-e). Furthermore, Western-blot analyses of roots from ELF4-GFP  
170 (Sh)/*elf4-1*(Rt) micrografts showed that ELF4 protein was effectively detected as a band of the  
171 expected size (arrows in Fig. 2i) not present in protein extracts of *elf4-1* mutant roots (Fig. 2i).  
172 Grafting ELF4-ox fused to three GFPs (ELF4-x3GFP) scion into *elf4-2* mutant rootstock did not  
173 lead to an obvious recovery of rhythms (Fig. 2j and Extended Data Fig. 5f) suggesting the  
174 requirement of a mobile ELF4 protein. The ELF4-x3GFP is still functional as its over-  
175 expression in the *elf4-1* mutant background restored the hypocotyl phenotypes of *elf4-1* mutant  
176 (Extended Data Fig. 5g) and repressed *PRR9* gene expression (Extended Data Fig. 5h-i). The

functional relevance of ELF4 movement was also verified in *elf4-1*(Sh)/*elf4-1*(Rt) grafts showing the lack of rhythmic recovery in *elf4-1* roots when *elf4-1* was used as scion (Extended Data Fig. 5j-k). Therefore, multiple series of evidence including the ELF4 injection data, the grafting assays showing the recovery of the rhythms, the ELF4-GFP fluorescent signals across the graft junctions, the detection of the ELF4 protein in roots of the grafted plants, the lack of rhythmic recovery in roots of ELF4-x3GFP and in *elf4-1* scion grafts, support the notion that ELF4 protein moves from shoots to regulate rhythms in roots. Other mobile proteins such as FT (FLOWERING LOCUS T), and HY5 (LONG HYPOCOTYL 5) share some features with ELF4 protein in terms of low molecular weight and high isoelectric point (Fig. 2k).

### Blocking ELF4 movement by shoot excision alters circadian rhythms in roots

We next attempted to unveil the function of the mobile ELF4 by blocking ELF4 movement through shoot excision. Analyses of the rhythms showed that excised roots sustained robust oscillations (Extended Data Fig. 6a-b) confirming that the root clock is able to run in the absence of shoots. However, comparison of intact versus excised roots uncovered a shorter period in excised roots (Extended Data Fig. 6c-d). As accumulation of ELF4 results in long periods in shoots<sup>22</sup> and roots (Fig. 1e and Extended Data Fig. 1k), it is plausible that blocking ELF4 movement by shoot excision leads to shorter periods in excised roots. If that is the case, blocking ELF4 movement should also affect ELF4 target gene expression in excised roots. Time course analyses by RT-QPCR revealed that the expression of *PRR9* and *PRR7* was up-regulated in excised roots compared to intact roots (Extended Data Fig. 6e-f), which suggest that in the absence of ELF4 movement from shoots, repression of these genes is alleviated in roots. The use of ELF4-ox intact roots confirmed that *PRR9* and *PRR7* are targets of ELF4 as their expression was clearly down-regulated in intact ELF4-ox roots compared to WT intact roots (Extended Data Fig. 6g-h). Furthermore, ELF4-ox excised roots still showed repression of target gene expression (Extended Data Fig. 6i-j) suggesting that excision *per se* is not responsible for the up-regulation observed in WT excised roots.

To further uncover the function of ELF4 movement, we performed RNA-Seq analyses of WT intact versus excised roots. Our results showed that as expected, a significant fraction of genes was affected by excision (Supplementary Table 2). Comparative analyses of *elf4-1* intact roots with WT excised roots allowed us to discern the effects due to excision from those due to the lack of ELF4 movement (Extended Data Fig. 7). Indeed, we focused on the differentially expressed genes (DEGs) present in both excised WT and intact *elf4-1* roots. As *elf4-1* mutant roots are intact, the overlapping DEGs are not affected by excision *per se* but rather by the lack of ELF4 movement from shoots, which is shared by *elf4-1* intact roots and WT excised roots.

Our comparative analyses of both datasets revealed that 67% of the DEGs in *elf4-1* intact roots are also differentially expressed in WT excised roots (Supplementary Table 3) (Extended Data Fig. 7). The proportion of overlapped DEGs (67%) is highly significant (P-value < 0.0001, chi-square test for equality of proportions) as compared to the proportion of overlapping genes (26%) using a random gene list. The overlap is noteworthy due to the different genotypes (*elf4-1* mutant versus WT) and most importantly, the different conditions (intact versus excised). As WT excised roots and *elf4-1* intact roots share the lack of ELF4 movement from shoots, the overlapping DEGs provides a hint about genes that directly or indirectly require ELF4 movement for proper expression in roots. Consistently, the overlap of DEGs included nearly all of the core oscillator genes (Supplementary Table 3 and Extended Data Fig. 6k). A significant fraction of overlapped DEGs also circadianly oscillated with phase enrichments during the subjective morning and subjective midday (Extended Data Fig. 6l). Therefore, ELF4 movement appears to be important for a fully functional clock in roots.

#### **Mobile ELF4 does not regulate the photoperiodic-dependent phase in roots**

In aerial tissues, the circadian clock controls the photoperiodic regulation of growth and development<sup>50</sup>. To determine whether ELF4 movement is important to deliver photoperiodic information, we analyzed rhythms under short day (ShD) and long day (LgD) conditions. In roots, *PRR9::LUC* waveforms displayed a subtle phase delay under LgD compared to ShD (Fig. 3a) following a similar trend to that observed in shoots (Fig. 3b). Time course analyses by Western-blot of roots of ELF4 Minigene plants<sup>20</sup> confirmed the phase delay of ELF4 protein accumulation under LgD compared to ShD (Fig. 3c-d). We reasoned that if ELF4 movement is correlated with the photoperiodic-dependent phase delay, then excision of shoots might affect the phase shift in roots. In agreement with the oscillations in promoter activity (Extended Data Fig. 6c-d), the phase of ELF4 protein accumulation was advanced following excision under both LgD and ShD (Extended Data Fig. 8a-d). Interestingly, under LgD conditions, excision rendered a similar pattern of ELF4 accumulation than in intact roots under ShD (Fig. 3e-f). Therefore, excision abolished the phase delay observed in intact root under LgD (compare Fig. 3c-d with Fig. 3e-f). The results suggest that the photoperiodic-dependent phase shift in roots is hampered by blocking ELF4 movement. However, excised roots still showed the phase delay under LgD compared to excised roots under ShD (Extended Data Fig. 8e-f). Furthermore, analyses of rhythms under LgD conditions showed that plants mis-expressing ELF4 (ELF4-ox and *elf4-1* mutant) displayed very similar rhythms to WT both in shoots and roots (Fig. 3g-h) suggesting that ELF4 function is not essential to sustain rhythms under entraining conditions. Together, the results suggest that blocking ELF4 movement by excision advances the phase of the root clock but the mobile ELF4 does not directly regulate the photoperiodic-dependent phase shift in roots.



250

251 **ELF4 movement contributes to the temperature-dependent changes in circadian period of**  
252 **the root clock**

253 As the EC also coordinates temperature responses, we examined whether a mobile ELF4 can  
254 convey temperature information from shoots to roots. To that end, we first examined the effect  
255 of different temperatures (28°C, 18°C and 12°C) on circadian rhythms in roots. We found that  
256 *LHY::LUC* circadian period length was shorter at high than at low temperatures (Extended Data  
257 Fig. 9a-b). Shortening of period length at increasing temperature was also observed for other  
258 circadian reporter lines (Extended Data Fig. 9c-f) indicating that at this developmental stage and  
259 under our experimental conditions, the circadian clock in roots is not able to perfectly sustain  
260 circadian period length within a range of temperatures.

261

262 As ELF4 accumulation lengthens period length, we next examined the possible contribution of  
263 ELF4 to the long period phenotype at low temperatures. Changes in period length could be  
264 mediated by increased ELF4 activity and/or by the increased protein movement from shoots to  
265 roots. To examine these possibilities, we compared the effects of blocking ELF4 movement by  
266 excision at low and high temperatures. Essentially, if the long period in roots at 12°C is  
267 independent of movement but results from the increased activity of ELF4, blocking movement  
268 from shoots by excision should not have a major effect on period length. However, if ELF4  
269 movement contributes to the period regulation, abolishing ELF4 traffic should lead to an  
270 observable and differential effect on period length at different temperatures.

271

272 Our results showed that excision shortened the period length in WT roots and this effect was  
273 significant at 12°C as compared to the minor effect at 28°C (Extended Data Fig. 10a-d).  
274 Therefore, blocking ELF4 movement by excision shortens the long period of WT roots at 12°C.  
275 Analyses of other circadian reporter lines and at 18°C also showed that excision shortened  
276 period length compared to intact roots (Extended Data Fig. 10e-f). The results suggest a  
277 temperature-dependent control of ELF4 movement that regulates period length in roots. To  
278 further verify this notion, we examined rhythmic recovery in grafts of ELF4-ox scion into *elf4-1*  
279 rootstock at low and high temperatures. Our results showed an evident rhythmic recovery at  
280 12°C but not at 28°C (Fig. 4a-b). Furthermore, grafts of E4MG scion into *elf4-1* rootstock also  
281 efficiently recovered rhythms at 12°C but not at 28°C (Fig. 4c-d). ELF4 is still able to delay the  
282 phase and lengthen the period at 28°C (Fig. 4e and Extended Data Fig. 10g) suggesting that  
283 movement rather than changes in activity are responsible for the observed effects. ELF4 protein  
284 accumulation in roots of ELF4-ox scion into *elf4-1* rootstock was higher at 12°C than at 28°C  
285 (Figure 4f and Extended Data Fig. 10h-i) but ELF4 (E4MG) protein accumulation in shoots is

286 similar at different temperatures<sup>31</sup> (Extended Data Fig. 10j). Therefore, ELF4 movement rather  
287 than protein accumulation or activity appears to be regulated by temperature, contributing to the  
288 temperature-dependent control of circadian period in roots.

289

290 Altogether, we propose a model by which mobile ELF4 (mbE4) from shoots to roots defines a  
291 pool of active ELF4 protein that is competent to repress target circadian gene expression in  
292 roots. ELF4 trafficking is favored at low temperatures, which results in a slow-paced clock (Fig.  
293 4g) while high temperatures decrease the movement, leading to a fast root clock (Fig. 4h). The  
294 temperature-dependent movement of ELF4 allows a shoot-to-root dialogue that controls the  
295 pace of the clock and provides a mechanism by which temperature cues from shoots set the  
296 circadian period length in roots.

297

## 298 **Discussion**

299 The simultaneous examination of rhythms in shoots and roots of single individual plants shows  
300 that the promoter activities and mRNA accumulation of clock genes in roots display a longer  
301 period and delayed phase compared to shoots. The trend was observed for morning- and  
302 evening-expressed key oscillator genes suggesting that the overall circadian system in roots is  
303 not as precise as in other parts of the plant (e.g. the shoot apex)<sup>47</sup>. Despite the long period, the  
304 rhythms persist in roots for several days under LL, which is reminiscent of a fully functional  
305 clock. The lack of precision might provide circadian flexibility for rapid adjustments and  
306 improved responses in roots. Previous studies have reported spatial waves of clock gene  
307 expression with and within organs<sup>40, 42, 45</sup> that might be due to differences in period length and  
308 variable local coupling.

309

310 The EC directly represses *PRR9* and *PRR7* expression<sup>19, 23, 29, 51, 52</sup> and indirectly promotes the  
311 expression of the morning-expressed oscillator genes *CCA1* and *LHY*<sup>51-54</sup>. Our analyses with  
312 *elf4-1* mutant and ELF4-ox plants demonstrate that ELF4 function in roots is also important for  
313 proper repression of *PRR9* and *PRR7* and activation of *CCA1* and *LHY*. ELF4 regulatory  
314 function in roots appears to be similar to that previously described for the EC using whole  
315 plants. Over-expression of ELF4 lengthens the period of the root clock suggesting that ELF4  
316 slows down the circadian period in roots as in shoots<sup>22</sup>. The fact that accumulation of ELF4  
317 lengthens the period agrees with the results showing that blocking movement by shoot excision  
318 shortens the period. RNA-Seq analyses revealed that not only the expression of oscillator genes  
319 is affected in *elf4-1* roots but also a battery of genes involved in other pathways including  
320 responses to stimuli. These pathways are also consistent with the EC function in responses to  
321 environmental cues<sup>55</sup>. The mis-regulated genes in *elf4-1* roots might be direct targets of ELF4

322 and/or indirect outputs of the clock in roots. One of these outputs might be lateral root  
323 emergence as the number of lateral roots is affected in *elf4-1* and ELF4-ox compared to WT.  
324 Future studies are necessary to uncover the molecular and cellular mechanisms by which ELF4  
325 regulates the number of lateral roots in Arabidopsis.

326  
327 Micrografts of ELF4-ox scion into *elf4-1* or *elf4-2* rootstocks allow a remarkable recovery of  
328 rhythms that is not observed when seedlings expressing ELF4 protein fused to 3 GFPs in  
329 tandem is used as scion. These results suggest that ELF4 movement is indeed important for the  
330 rhythmic recovery. Fluorescent signals accumulating in the vasculature of *elf4-1* mutant  
331 rootstock grafted with ELF4-GFP scion and the detection of the ELF4 protein in roots of the  
332 micrografted plants also suggest that ELF4 moves from shoots to roots. This conclusion is  
333 complemented with the grafting assays of *elf4-1*(Sh)/*elf4-1*(Rt) showing the lack of rhythmic  
334 recovery in roots, and with the assays of ELF4 protein injection in shoots and the subsequent  
335 rhythmic recovery in roots. Micrografts of E4MG and WT plants are also able to recover the  
336 rhythms of the *elf4-1* mutant roots, which indicate that the effects are not due to the over-  
337 accumulation of ELF4-ox and suggest that the amount of mobile ELF4 that is required to  
338 regulate the rhythms is probably not very high. Our experiments adding water to the scion or  
339 using WT scion without LUC reporter exclude the possibility that rhythms in grafted roots are  
340 due to leakage for the adjacent well containing the shoot. The fact that ELF4 protein shows  
341 similar properties in terms of length, molecular weight and isoelectric point to other mobile  
342 proteins<sup>56-59</sup> also support the notion of ELF4 movement. We postulate that following movement,  
343 the complex regulatory feedback loops at the core of the oscillator will be reset to control the  
344 pace of the clock. Further experiments at different developmental stages and various growing  
345 conditions (e.g. light and temperature) will be required to confirm whether the long distance  
346 movement of ELF4 contributes or not to the spatial waves of clock gene expression observed in  
347 roots<sup>42</sup>.

348  
349 Excision blocks ELF4 movement from shoots and consequently, we observe that oscillator gene  
350 expression and other output genes are affected in WT excised roots. Previous studies have also  
351 used excision to define properties of the circadian function in roots<sup>42</sup>. Although many genes are  
352 affected by excision, it is noteworthy that 67% of the genes mis-regulated in *elf4-1* intact roots  
353 are also mis-expressed in WT excised roots. Both conditions share the lack of ELF4 movement,  
354 which suggest that the overlapped DEGs are due to the lack of a mobile ELF4 (note that the  
355 RNA-Seq studies with *elf4-1* mutant were performed with intact roots). The phase shifts  
356 observed following excision prompted us to examine whether ELF4 movement contributed to  
357 the photoperiodic-dependent phase shift. However, excised roots still sustained the phase delay  
358 under LgD suggesting that other factors are responsible for this regulation. Light piping down

the root<sup>49</sup> might be also important for synchronization. Regardless the mechanism, it is able to overcome the mis-expression of ELF4 in shoots and roots as ELF4-ox and *elf4-1* mutant plants displayed similar rhythms to WT. Clear alteration of circadian expression under LL but not under entraining conditions has been reported for other clock mutants and over-expressing plants<sup>60</sup>.

The EC activity is down-regulated at high temperatures in whole seedlings<sup>29, 31</sup>. Shoot excision shortened the period, suggesting that ELF4 movement is important in the control of circadian period length. Period shortening is more significant at low than at high temperatures confirming that ELF4 movement might be favored at low temperatures. The temperature-dependent control of ELF4 movement is also supported by the increased accumulation ELF4 protein in grafted roots at 12°C compared to 28°C. As ELF4 accumulation results in long period, the increased movement leads to a clock that runs slower at low than at high temperatures. It would be interesting to elucidate whether period sensitivity to temperature might provide an advantage for optimal root responsiveness to temperature variations.

## Methods

### Plant material, growth conditions, constructs and physiological assays

*Arabidopsis thaliana* seedlings were stratified at 4°C in the dark for 2-3 days on Murashige and Skoog (MS) agar medium with 3% of sucrose (MS3). Plates were transferred to chambers with light- and temperature-controlled conditions with 25-50  $\mu\text{mol}\cdot\text{quanta}\cdot\text{m}^{-2}\cdot\text{s}^{-1}$  of cool white fluorescent light. Seedlings were synchronized under Light:Dark cycles, LD (12h light: 12h dark) at 22°C. For experiments with different temperatures, seedlings were analyzed under constant light conditions at 12°C, 18°C, 22°C or 28°C following synchronization under LD (12h light: 12h dark) at 22°C. For experiments with different photoperiods, seedlings were grown under short days (ShD, 8h light: 16h dark) or long days (LgD, 16h light: 8h dark). Reporter lines *CCA1::LUC*<sup>61</sup>, *LHY::LUC*<sup>19</sup>, *PRR9::LUC*<sup>62</sup>, *TOC1::LUC*<sup>6</sup> and *elf4-1*<sup>17</sup>, *elf4-2*<sup>27</sup>, ELF4 Minigene<sup>20</sup> and ELF4-GFP-ox<sup>19, 20</sup> plants were described elsewhere. The ELF4 construct fused to three Green Fluorescent Proteins (GFPs) in tandem was generated by PCR-mediated amplification of the *ELF4* coding sequence and subsequent subcloning into the PGWB514 gateway vector<sup>63, 64</sup>. The resulting plasmid was digested with PacI and SacI restriction enzymes and ligated with the 3 GFPs insert from the pBS-x3GFP vector (Addgene). The construct was transformed into *elf4-1* mutant plants. Plants were transformed using *Agrobacterium tumefaciens* (GV2260)-mediated DNA transfer<sup>65</sup>. For in vitro protein injection assays, the ELF4 coding sequence was subcloned into the pET MBP\_1a vector (Novagen) after removing the GFP by Nco I and Xho I restriction enzyme digestion.

For lateral root analyses, WT, *elf4-1* and ELF4-ox seeds were surface-sterilized and plated onto MS medium supplemented with 0.25% w/v sucrose and 1.5% agar. The top quarter of the agar was removed and seeds pipetted evenly along this line. Plants were then grown vertically for 12 days before lateral roots were measured. Lateral roots were manually counted using a Nikon SMZ800 dissecting microscope. Statistical analysis was completed using R (version 3.6), within the R studio software package (version 1.1.4). For hypocotyl elongation measurements, WT, *elf4-1*, ELF4-GFP-ox and ELF4-3xGFP-ox seeds transformed into the *elf4-1* mutant background were stratified on MS3 medium in the dark for 4 days at 4°C, exposed to white light (40  $\mu\text{mol}\cdot\text{quanta}\cdot\text{m}^{-2}\cdot\text{s}^{-1}$ ) for 6 h and maintained in the dark (22°C) for 18 h before transferring to chambers under Short-Day conditions (8h light:16h dark). Hypocotyl length was measured using the ImageJ software (version 1.48v) (<https://imagej.nih.gov/ij/>) at 7 days after stratification. Each experiment was repeated at least twice using 20-50 seedlings per genotype. Statistical analyses were performed using the GraphPad Prism software (version 5.01; GraphPad Software, Inc) using two-tailed t-tests with 95% of confidence.

#### **In vivo luminescence assays**

In vivo luminescence assays were performed as previously described<sup>47</sup>. Briefly, 7-15 day-old seedlings synchronized under LD cycles at 22°C were transferred to 96-well plates and released into the different conditions as specific for each experiment. Analyses were performed with a LB960 luminometer (Berthold Technologies) using the Microwin software (Version 4.41; Mikrotek Laborsysteme). The period, phase and amplitude were estimated using the Fast Fourier Transform–Non-Linear Least Squares (FFT–NLLS) suite<sup>66</sup> using the Biological Rhythms Analysis Software System (version 3.0; BRASS, <http://www.amillar.org>). For the simultaneous analysis of rhythms of shoots and roots from the same plant, the connection between the two adjacent wells of the 96-well plates was serrated. Seedlings were then horizontally positioned so the shoot was placed in one well and the roots in the contiguous well. For excision analyses, roots were excised from shoots and placed into the 96-well plates for luminescence analyses. Data from samples that appeared damaged or contaminated were excluded from the analysis. For analyses of grafted samples, water instead of luciferin was applied to the wells containing shoots to avoid possible leaking signals from shoots to roots as specified. At least two biological replicates were performed per experiment, with measurements taken from distinct samples grown and processed at different times. Each biological replicate included 6 to 12 independent seedlings per condition and/or genotype. Statistical analyses were performed using the GraphPad Prism software (version 5.01; GraphPad Software, Inc) using two-tailed t-tests with 95% of confidence.

432

### 433 **Protein purification and injection analyses**

434 *E. coli* cells (BL21, Dh5α) were transformed and grown in LB medium (Tryptone 10 g/L, yeast  
 435 extract 5 g/L, NaCl 10 g/L pH 7.5) until OD600 values of 0.8-1.0. Isopropyl β-D-1-  
 436 thiogalactopyranoside (IPTG)-mediated induction of MBP-ELF4 and MBP-GFP was performed  
 437 at 28°C for 6 h. Bacteria resuspended in lysis buffer (50mM Tris-HCl, pH7-8, 5% glycerol,  
 438 50mM NaCl) were lysed by sonication for 2-3 minutes (30s on, 30s off, high intensity) using a  
 439 sonicator (Bioruptor, Diagenode). Recombinant proteins were purified using gravity flow  
 440 columns with amylose resin (New England Biolabs). MBP cleavage was performed by  
 441 incubation in cleavage buffer (50 mM Trizma-HCl, pH 8.0, 0.5 mM EDTA, and 1 mM DTT)  
 442 for 2 hours at 30°C with native Tobacco Etch Virus (TEV) protease (Sigma-Aldrich). The  
 443 purified recombinant proteins were concentrated using Amicon centrifugal filters following the  
 444 manufacturer recommendations (Millipore). Protein yield was estimated by measuring  
 445 absorbance at 595 nm using a spectrophotometer (UV-2600, SHIMADZU). Proteins were also  
 446 examined by Coomassie-Brilliant Blue staining of polyacrylamide gels to confirm protein size  
 447 and integrity. Purified ELF4 was injected into leaves of 10-day old *elf4-1* mutant seedlings  
 448 harboring the *LHY::LUC* reporter line. Similar concentration of GFP protein was also injected  
 449 as a negative control. Rhythms were subsequently examined in a LB960 luminometer (Berthold  
 450 Technologies) as described above.

451

### 452 **Time course analyses of gene expression by RT-qPCR**

453 Seedlings were synchronized under LD cycles in MS3 medium plates for 12-14 days and  
 454 subsequently transferred to LL. Shoots and roots from intact plants were taken every 4 hour  
 455 over the circadian cycle. For excised roots, shoots and roots were carefully separated with a  
 456 sterile razor blade and the excised roots were deposited on MS3 agar medium plates for 2 or 3  
 457 days as specified. RNA was purified using a Maxwell RSC Plant RNA kit following the  
 458 manufacturer's recommendations (Promega). Single-stranded cDNA was synthesized using  
 459 iScript Reverse Transcription Supermix for RT-qPCR (Bio-Rad). qPCR analyses were  
 460 performed with cDNAs diluted 50-fold with nuclease-free water using Brilliant III Ultra-Fast  
 461 SYBR Green qPCR Master Mix (Agilent) with a 96-well CFX96 Touch Real-Time PCR  
 462 detection system (Bio-RAD CFX96 Manager version 3.1, Bio-Rad). Each sample was run in  
 463 technical triplicates. The expression of *PP2AA3* (*PROTEIN PHOSPHATASE 2A SUBUNIT A3*,  
 464 *AT1G13320*) or *MON1* (*MONENSIN SENSITIVITY1*, *AT2G28390*)<sup>67</sup> was used as a control.  
 465 Crossing point (Cp) calculation was used for quantification using the Absolute Quantification  
 466 analysis by the 2<sup>nd</sup> Derivative Maximum method. At least two biological replicates were

performed, with measurements taken from distinct samples grown and processed at different times.

#### RNA-Seq analyses

Roots from 14-day old intact WT, *elf4-1* mutant and excised WT plants synchronized under LD cycles in MS3 medium plates were transferred to LL conditions for 3 days. Roots were excised just before transferring to LL. Samples were collected at the fourth day under LL at circadian time 75 (CT75). Total RNA was isolated using a Maxwell RSC Plant RNA kit. RNA sequencing was performed by IGATech (Italy). About 1-2 µg of high quality RNA (R.I.N. >7) was used for library preparation with a TruSeq Stranded mRNA Sample Prep kit (Illumina, San Diego, CA). Poly-A mRNA was fragmented for 3 minutes at 94°C. Purification was performed with 0.8x Agencourt AMPure XP beads. Both RNA samples and final libraries were quantified using the Qubit 2.0 Fluorometer (Invitrogen, Carlsbad, CA). Quality was tested using the Agilent 2100 Bioanalyzer RNA Nano assay (Agilent technologies, Santa Clara, CA). Libraries were then processed with Illumina cBot for cluster generation on the flowcell, following the manufacturer's instructions and sequenced on paired-end mode at the multiplexing level requested on HiSeq2500 (Illumina, San Diego, CA). The CASAVA (1.8.2 version) of the Illumina pipeline was used to process raw data for both format conversion and de-multiplexing.

Sequence analysis was performed using the A.I.R. software (version 1.0) (<https://transcriptomics.sequentiabiotech.com/>) developed by Sequentia Biotech. Briefly, raw sequence files were first subjected to quality control analysis by using FastQC (v0.10.1) before trimming and removal of adapters with BBDuk (<https://jgi.doe.gov/data-and-tools/bbtools/>). Reads were then mapped against the *Arabidopsis thaliana* genome (TAIR10 Genome Release, <ftp://ftp.arabidopsis.org/>) with STAR (version 2.6)<sup>68</sup>. FeatureCounts (version 1.6.1)<sup>69</sup> was then used to obtain raw expression counts for each annotated gene. The differential expression analysis was conducted with edgeR (version 3.18.1)<sup>70</sup>, using the TMM normalization method. FPKM were obtained with edgeR.

The Integrative Genomics Viewer (IGV, version 2.4.13) (<https://software.broadinstitute.org/software/igv/>) was used to visualize the data<sup>74, 75</sup>. The circadian phases were analyzed using the publicly available Gene Phase Analysis Tool "PHASER" of the DIURNAL database (<http://diurnal.mocklerlab.org/>)<sup>76, 77</sup>. Phase over-representation is calculated as the number of genes with a given phase divided by the total number of genes over the number of genes called rhythmic and divided by the total number of genes in the dataset. Functional categories of the DEG were obtained using the web tool "BIOMAPS"(VirtualPlant, version 1.3)<sup>78</sup>, which renders over-represented and significant

functional terms (Gene Ontology or MIPS) as compared to the frequency of the term in the whole genome.

#### **Western-blot assays**

Approximately 50-100 mgs of roots from plants grown under the specified photoperiodic condition were sampled every four hours over a 24-hour cycle. Samples were rapidly frozen with liquid nitrogen and grounded with stainless steel beads (Millipore) in a tissue lyser (QIAGEN, TissueLyser II). Tissue was subsequently resuspended in Protein Extraction Buffer (PEB) containing 50 mM Tris-HCl pH 7.5, 150 mM NaCl, 0.5% NP40, 1 mM EDTA, and protease inhibitors cocktail (1:100) and PMSF (1:1000). Protein extracts were centrifuged at 4 °C, measured for protein concentration using Bradford reagent (Bio-Rad) and normalized to 2 mg/ml in 4 x SDS loading buffer (250 mM Tris-HCl, pH 6.8, 8% SDS, 0.08% bromophenol blue, 40% glycerol). Samples were run on a 12% gel and analyzed by immunoblotting, fixed 30 min with 0.4% Glutaraldehyde solution (Sigma-Aldrich) and detected with an anti-HA antibody (Roche) (1:2000 dilution) and a goat anti-rat horse peroxidase conjugated secondary antibody (Sigma-Aldrich) (1:4000 dilution). For analyses of the grafted plants, roots from plants synchronized under LD cycles were subsequently transferred to LL for 3 days at 12°C, 22°C or 28°C. Samples were collected at CT81, rapidly frozen with liquid nitrogen and grounded with stainless steel beads (Millipore) in a tissue lyser (QIAGEN, TissueLyser II). Powder extracts were subsequently resuspended in Protein Extraction Buffer (PEB) containing 50 mM Tris-HCl pH 7.5, 150 mM NaCl, 0.5% NP40, 1 mM EDTA, and protease inhibitors cocktail (1:100), PMSF (1:1000), and MG132 (100uM). Protein extracts were centrifuged at 4 °C, measured for protein concentration using Bradford reagent (Bio-Rad) and normalized to 2 µg/µl in 4 x SDS loading buffer (250 mM Tris-HCl, pH 6.8, 8% SDS, 0.08% bromophenol blue, 40% glycerol and 5 mM β-mercaptoethanol). For detection of ELF4 protein fused to GFP, samples were run on a 10% gel and was detected using an anti-GFP antibody (ab290, Abcam) (1:5000) and Goat anti-Rabbit IgG (H+L) Secondary Antibody, HRP (31460, Lot: OG188649, Thermo Fisher Scientific) (1:5000 dilution). For detection of ELF4 protein fused to HA (ELF4 Minigene) in shoots, samples were resuspended in Protein Extraction Buffer (PEB) containing 50mM TrisHCl pH7.5, 150mM NaCl, 0.5% NP40, 1mM EDTA, protease inhibitors and proteasome inhibitor (MG132, 100uM). Protein extracts in 4× SDS loading buffer (250 mM Tris-HCl, pH 6.8, 8% SDS, 0.08% bromophenol blue, 40% glycerol, 5 mM β-mercaptoethanol) were run on a 12% gel and analyzed by immunoblotting, fixed 30 min with 0.4% Glutaraldehyde solution (Sigma-Aldrich) and detected with an Anti-HA antibody High Affinity from rat IgG1 (11867423001, Sigma-Aldrich) (1:2000) and a goat anti-rat horse peroxidase conjugated secondary antibody (A9037, Sigma-Aldrich) (1:4000). The Image Lab software (version 5.2.1; Bio-Rad) was used to image the Western-blots. Membranes were stained with a Ponceau S



541 solution following the manufacturer recommendations (Sigma). Proteins were also run on a  
 542 10% SDS-PAGE gel and stained with Coomassie-Brilliant Blue. At least two biological  
 543 replicates were performed per experiment and/or condition, with measurements taken from  
 544 distinct samples grown and processed at different times.

545

#### 546 **Micrografting assays**

547 Micrografting was performed essentially as previously described<sup>47</sup>. Data from unsuccessful  
 548 grafted seedlings that failed to properly join together or grafts that were insufficiently clear to be  
 549 successful were discarded. Approximately 100-150 grafting events were performed for every  
 550 combination of grafts. The percentage of successfully micrografted plants was about 30-50 %  
 551 (possibly higher but only the clearly successful grafted plants were taken into account). From  
 552 the successfully grafted plants, 30-60 % showed different degrees of recovered rhythms. For in  
 553 vivo luminescence assays, shoots and roots of grafted plants were simultaneously examined  
 554 using the protocol described above. Water instead of luciferin was added to the wells containing  
 555 shoots to exclude the possibility that recovery of rhythms in roots were due to leaking signals  
 556 from shoots. As specified, some grafted shoots contained no reporter fused to luciferase.

557

#### 558 **Reconstruction of driving forces by recurrence plots**

559 Common driving forces were estimated following a several-step procedure. Suppose that we  
 560 have the number  $K$  of simultaneous time series measurements  $\{s_i(t)|i = 1, 2, \dots, K, t =$   
 561  $1, 2, \dots, T\}$ . First, we took time differences  $\tilde{s}_i(t) = s_i(t + 1) - s_i(t)$  ( $i = 1, 2, \dots, K, t =$   
 562  $1, 2, \dots, T - 1$ ) of consecutive measurements and remove trends. Second, we used delay  
 563 coordinates<sup>79, 80</sup>  $\vec{s}_i(t) = [\tilde{s}_i(t), \tilde{s}_i(t + 1), \tilde{s}_i(t + 2), \tilde{s}_i(t + 3), \tilde{s}_i(t + 4)]$  of 5 dimensional space  
 564 ( $i = 1, 2, \dots, K, t = 1, 2, \dots, T - 4$ ) to obtain a recurrence plot<sup>81</sup>. A recurrence plot is a two-  
 565 dimensional figure proposed originally for visualizing time series data. Both axes are the same  
 566 time axis. If the Euclidean distance  $\|\vec{s}_i(t_1) - \vec{s}_i(t_2)\| < \varepsilon_i$ , where  $\varepsilon_i$  is a threshold and  $t_1, t_2 \in$   
 567  $\{1, 2, \dots, T - 4\}$ , then we plot a point at  $(t_1, t_2)$ . We denote this as  $R_i(t_1, t_2) = 1$ . Otherwise, we  
 568 do not plot a point at  $(t_1, t_2)$ . We denote this state as  $R_i(t_1, t_2) = 0$ . We controlled the value of  
 569 the threshold  $\varepsilon_i$  for each component  $i \in \{1, 2, \dots, K\}$  so that 5% points, except for the central  
 570 diagonal line, have points plotted. Third, we took the union for the recurrence plots to infer the  
 571 recurrence plot of the common driving force<sup>82</sup>. Namely we declare  $R(t_1, t_2) = 1$  if we have  
 572  $R_i(t_1, t_2) = 1$  for at least one of  $i \in \{1, 2, \dots, K\}$ . Otherwise, we have  $R(t_1, t_2) = 0$ . In each of  
 573 the original recurrence plots, points are plotted where the driving force and the driven system  
 574 are both similar. By taking their union, we can extract pairs of times where only the driving  
 575 force is similar. Fourth, we applied the assumption of continuity and supplied the points at  
 576  $(t, t+1)$  and  $(t+1, t)$  for each  $i$ <sup>83</sup>. Namely, we forcefully declare  $R(t, t + 1) = R(t + 1, t) = 1$  for

577  $t = 1, 2, \dots, T - 5$ . Fifth, we applied the method described<sup>82</sup> to convert the recurrence plot of the  
578 common driving force into time series. Here we describe the detail for this step: (i) we construct  
579 a network where each node correspond to a time point and we connect two nodes  $t_1$  and  $t_2$  if  
580  $R(t_1, t_2) = 1$ ; (ii) we assign a distance for each edge as  $1 - \frac{\#\{k=1,2,\dots,T-4|R(k,t_1)=1 \text{ and } R(k,t_2)=1\}}{\#\{k=1,2,\dots,T-4|R(k,t_1)=1 \text{ or } R(k,t_2)=1\}}$ ,  
581 (iii) we obtain the shortest distance for each pair of nodes on this graph (this process  
582 approximates the geodesic distance between two time points); (iv) we apply the multi-  
583 dimensional scaling to convert the distance matrix to a time series. Namely this fifth step works  
584 as the inverse transform of a recurrence plot and we can reproduce a rough shape for the  
585 original time series. This fifth step has two mathematical proofs<sup>84, 85</sup>. Lastly, we extracted the  
586 component corresponding to the largest eigenvalue. The periodicity of the reconstructed  
587 common driving force  $X(t)$  was evaluated using the autocorrelation function and 10000 random  
588 shuffle surrogates<sup>86</sup>, for each of which the order of time points is randomly exchanged. Here, the  
589 null hypothesis was that there was no serial dependence. The autocorrelation with time  
590 difference  $k$  is the correlation coefficient between  $X(t)$  and  $X(t+k)$ . Thus, it is close to 1 if  $X(t)$   
591 and  $X(t+k)$  are similar while it is close to 0 if they are not related to each other. If there is a 24h  
592 periodicity in the driving force, the autocorrelation with 24h time difference should be a value  
593 close to 1.

#### 594 **Confocal imaging**

595 For *in vivo* confocal imaging, the roots of WT and ELF4-ox (fused to GFP) grafted shoots into  
596 *elf4-1* mutants were placed on microscope slides (Sigma). Fluorescent signals were imaged with  
597 an argon laser (transmissivity: 40%; excitation: 515 nm; emission range: 530–630 nm) in a  
598 FV1000 confocal microscope (Olympus, Tokyo, Japan) using a FV-10-ASW4.2 Viewer  
599 Manager software (Olympus) with a 40x/1.3 oil immersion objective. The image sizes were  
600 about 640 x 640 (0.497  $\mu\text{m}/\text{pixel}$ ) and sampling speed of 4  $\mu\text{s}/\text{pixel}$ . The results are  
601 representative of at least three biological replicates for grafting and about three-four images per  
602 grafts.

604 **List of primers.** List of primers used for expression analyses, cloning and generation of 3x GFP  
605 construct.

Name	Sequence	Experiment
REF1(PP2A_A3)_EXP_F	AAGCGTTGTGGAGAACATGATACG	Expression analysis
REF1(PP2A_A3)_EXP_R	TGGAGAGCTTGATTTGCGAAATACCG	Expression analysis
MON1_EXP_F	AACTCTATGCAGCATTTGATCCACT	Expression analysis
MON1_EXP_R	TGATTGCATATCTTTATCGCCATC	Expression analysis
PRR7_EXP_F	AAGTAGTGATGGGAGTGGCG	Expression analysis
PRR7_EXP_R	GAGATACCGCTCGTGGACTG	Expression analysis
PRR9_EXP_F	ACCAATGAGGGGATTGCTGG	Expression analysis

PRR9_EXP_R	TGCAGCTTCTCTCTGGCTTC	Expression analysis
ELF4_EXP_F	GACAATCACCAATCGAGAAT	Expression analysis
ELF4_EXP_R	ATGTTTCCGTTGAGTTCTTG	Expression analysis
CCA1_EXP_F	TCGAAAGACGGGAAGTGAACG	Expression analysis
CCA1_EXP_R	GTCGATCTTCATTGGCCATCTCAG	Expression analysis
LHY_EXP_F	AAGTCTCCGAAGAGGGTCGT	Expression analysis
LHY_EXP_R	GGCGAAAAGCTTTGAGGCAA	Expression analysis
ELF4_CLN_F	CACCATGAAGAGGAACGGCGA	Cloning
ELF4_CLN_R	AGCTCTAGTTCCGGCAGCACCA	Cloning
MBP-ELF4_CLN_F	CATGCCATGGGCATGAAGAGGAACGGCGAG	Cloning
MBP-ELF4_CLN_R	CCGCTCGAGTTAAGCTCTAGTTCCGGCAGCAC	Cloning
PacI-pBS3xGFP-F	GGTTAATTAACGCTGGAGGATCCATGTCTA	Generation of pGWB-c3xGFP
SacI-pBS3xGFP-R	TCGAGCTCTCTAGAACTAGTGGATCTTTA	Generation of pGWB-c3xGFP

606

607

608 **Reporting Summary.** Further information on research design is available in the Nature  
609 Research Reporting Summary linked to this article.

610

#### 611 **Data availability**

612 Data and materials generated in this study are available without restriction and should be  
613 requested to Paloma Mas: [paloma.mas@cragenomica.es](mailto:paloma.mas@cragenomica.es). NGS data are deposited in NCBI with  
614 accession code PRJNA610472 (BioSample accessions SAMN14299292, SAMN14299293,  
615 SAMN14299294). Source data are provided for all figures.

616

#### 617 **References**

- 618 1. Zhang, E.E. & Kay, S.A. Clocks not winding down: unravelling circadian networks.  
619 *Nat. Rev. Mol. Cell. Biol.* **11**, 764-776 (2010).
- 620 2. Greenham, K. & McClung, C.R. Integrating circadian dynamics with physiological  
621 processes in plants. *Nat. Rev. Genet.* **16**, 598-610 (2015).
- 622 3. Nagel, Dawn H. & Kay, Steve A. Complexity in the wiring and regulation of plant  
623 circadian networks. *Curr. Biol.* **22**, R648-R657 (2012).
- 624 4. Oakenfull, R.J. & Davis, S.J. Shining a light on the Arabidopsis circadian clock. *Plant*  
625 *Cell Environ* **40**, 2571-2585 (2017).
- 626 5. Hogenesch, J.B. & Ueda, H.R. Understanding systems-level properties: timely stories  
627 from the study of clocks. *Nature Reviews Genetics* **12**, 407 (2011).
- 628 6. Portolés, S. & Más, P. The functional interplay between protein kinase CK2 and CCA1  
629 transcriptional activity is essential for clock temperature compensation in Arabidopsis.  
630 *PLoS Genetics* **6**, e1001201 (2010).
- 631 7. Hansen, L.L., van den Burg, H.A. & van Ooijen, G. Sumoylation Contributes to  
632 Timekeeping and Temperature Compensation of the Plant Circadian Clock. *J Biol*  
633 *Rhythms* **32**, 560-569 (2017).
- 634 8. Marshall, C.M., Tartaglio, V., Duarte, M. & Harmon, F.G. The Arabidopsis *sickle*  
635 Mutant Exhibits Altered Circadian Clock Responses to Cool Temperatures and  
636 Temperature-Dependent Alternative Splicing. **28**, 2560-2575 (2016).

- 637 9. Salomé, P., Weigel, D. & McClung, C. The role of the Arabidopsis morning loop  
638 components CCA1, LHY, PRR7, and PRR9 in temperature compensation. *Plant Cell*  
639 **22**, 3650-3661 (2010).
- 640 10. Edwards, K.D., Lynn, J.R., Gyula, P., Nagy, F. & Millar, A.J. Natural allelic variation  
641 in the temperature-compensation mechanisms of the *Arabidopsis thaliana* circadian  
642 clock. *Genetics* **170**, 387-400 (2005).
- 643 11. Edwards, K.D. *et al.* FLOWERING LOCUS C mediates natural variation in the high-  
644 temperature response of the Arabidopsis circadian clock. *Plant Cell* **18**, 639 - 650  
645 (2006).
- 646 12. Ito, S. *et al.* FLOWERING BHLH transcriptional activators control expression of the  
647 photoperiodic flowering regulator *CONSTANS* in Arabidopsis. **109**, 3582-3587 (2012).
- 648 13. Gould, P.D. *et al.* Network balance via CRY signalling controls the Arabidopsis  
649 circadian clock over ambient temperatures. **9**, 650 (2013).
- 650 14. Nagel, D.H., Pruneda-Paz, J.L. & Kay, S.A. FBH1 affects warm temperature responses  
651 in the Arabidopsis circadian clock. **111**, 14595-14600 (2014).
- 652 15. Jones, M.A., Morohashi, K., Grotewold, E. & Harmer, S.L. Arabidopsis JMJD5/JMJ30  
653 Acts Independently of LUX ARRHYTHMO Within the Plant Circadian Clock to  
654 Enable Temperature Compensation. **10** (2019).
- 655 16. Gould, P.D. *et al.* The molecular basis of temperature compensation in the Arabidopsis  
656 circadian clock. *Plant Cell* **18**, 1177-1187 (2006).
- 657 17. Doyle, M.R. *et al.* The ELF4 gene controls circadian rhythms and flowering time in  
658 *Arabidopsis thaliana*. *Nature* **419**, 74-77 (2002).
- 659 18. Kolmos, E. *et al.* Integrating ELF4 into the circadian system through combined  
660 structural and functional studies. *HFSP journal* **3**, 350-366 (2009).
- 661 19. Herrero, E. *et al.* EARLY FLOWERING4 recruitment of EARLY FLOWERING3 in  
662 the nucleus sustains the Arabidopsis circadian clock. *Plant Cell* **24**, 428-443 (2012).
- 663 20. Nusinow, D.A. *et al.* The ELF4-ELF3-LUX complex links the circadian clock to  
664 diurnal control of hypocotyl growth. *Nature* **475**, 398-402 (2011).
- 665 21. Khanna, R., Kikis, E.A. & Quail, P.H. EARLY FLOWERING 4 functions in  
666 phytochrome B-regulated seedling de-etiolation. *Plant Physiol.* **133**, 1530-1538 (2003).
- 667 22. McWatters, H.G. *et al.* ELF4 is required for oscillatory properties of the circadian  
668 clock. *Plant Physiol.* **144**, 391-401 (2007).
- 669 23. Helfer, A. *et al.* LUX ARRHYTHMO encodes a nighttime repressor of circadian gene  
670 expression in the Arabidopsis core clock. *Curr. Biol.* **21**, 126-133 (2011).
- 671 24. Onai, K. & Ishiura, M. PHYTOCLOCK 1 encoding a novel GARP protein essential for  
672 the Arabidopsis circadian clock. *Genes Cells* **10**, 963-972 (2005).
- 673 25. Hazen, S.P. *et al.* LUX ARRHYTHMO encodes a Myb domain protein essential for  
674 circadian rhythms. *Proc. Natl. Acad. Sci. USA* **102**, 10387-10392 (2005).
- 675 26. Hicks, K.A. *et al.* Conditional circadian dysfunction of the *Arabidopsis early-flowering*  
676 *3* mutant. *Science* **274**, 790-792 (1996).
- 677 27. Huang, H. *et al.* Identification of Evening Complex associated proteins in Arabidopsis  
678 by affinity purification and mass spectrometry. *M. Cell. Proteomics* **15**, 201-217 (2016).
- 679 28. Li, G. *et al.* Coordinated transcriptional regulation underlying the circadian clock in  
680 Arabidopsis. *Nat. Cell Biol.* **13**, 616-622 (2011).
- 681 29. Mizuno, T. *et al.* Ambient temperature signal feeds into the circadian clock  
682 transcriptional circuitry through the EC night-time repressor in Arabidopsis thaliana.  
683 *Plant Cell Physiol.* **55**, 958-976 (2014).
- 684 30. Siddiqui, H., Khan, S., Rhodes, B.M. & Devlin, P.F. FHY3 and FAR1 act downstream  
685 of light stable phytochromes. *Front Plant Sci.* **7**, 175 (2016).
- 686 31. Ezer, D. *et al.* The evening complex coordinates environmental and endogenous signals  
687 in Arabidopsis. *Nat. Plants* **3**, 17087 (2017).
- 688 32. Kim, Y. *et al.* ELF4 Regulates GIGANTEA Chromatin Access through Subnuclear  
689 Sequestration. *Cell Reports* **3**, 671-677 (2013).

- 690 33. Nieto, C., López-Salmerón, V., Davière, J.-M. & Prat, S. ELF3-PIF4 Interaction  
691 Regulates Plant Growth Independently of the Evening Complex. *Current Biology* **25**,  
692 187-193 (2015).
- 693 34. Sai, J. & Johnson, C.H. Different circadian oscillators control Ca(2+) fluxes and lhcb  
694 gene expression. *Proc. Natl. Acad. Sci. USA* **96**, 11659-11663 (1999).
- 695 35. Thain, S.C., Murtas, G., Lynn, J.R., McGrath, R.B. & Millar, A.J. The circadian clock  
696 that controls gene expression in Arabidopsis is tissue specific. *Plant Physiol.* **130**, 102-  
697 110 (2002).
- 698 36. Michael, T.P., Salome, P.A. & McClung, C.R. Two Arabidopsis circadian oscillators  
699 can be distinguished by differential temperature sensitivity. *Proc. Natl. Acad. Sci. USA*  
700 **100**, 6878-6883 (2003).
- 701 37. Bordage, S., Sullivan, S., Laird, J., Millar, A.J. & Nimmo, H.G. Organ specificity in the  
702 plant circadian system is explained by different light inputs to the shoot and root clocks.  
703 *New Phytol.* **212**, 136-149 (2016).
- 704 38. Muranaka, T. & Oyama, T. Heterogeneity of cellular circadian clocks in intact plants  
705 and its correction under light-dark cycles. *Sci. Adv.* **2**, e1600500 (2016).
- 706 39. Thain, S.C., Hall, A. & Millar, A.J. Functional independence of circadian clocks that  
707 regulate plant gene expression. *Curr. Biol.* **10**, 951-956 (2000).
- 708 40. Fukuda, H., Nakamichi, N., Hisatsune, M., Murase, H. & Mizuno, T. Synchronization  
709 of plant circadian oscillators with a phase delay effect of the vein network. *Phys. Rev.*  
710 *Lett.* **99**, 098102 (2007).
- 711 41. Wenden, B., Toner, D.L.K., Hodge, S.K., Grima, R. & Millar, A.J. Spontaneous  
712 spatiotemporal waves of gene expression from biological clocks in the leaf. *Proc. Natl.*  
713 *Acad. Sci.* **109**, 6757-6762 (2012).
- 714 42. Greenwood, M., Domijan, M., Gould, P.D., Hall, A.J.W. & Locke, J.C.W. Coordinated  
715 circadian timing through the integration of local inputs in Arabidopsis thaliana. *PLOS*  
716 *Biology* **17**, e3000407 (2019).
- 717 43. Endo, M., Shimizu, H., Nohales, M.A., Araki, T. & Kay, S.A. Tissue-specific clocks in  
718 Arabidopsis show asymmetric coupling. *Nature* **515**, 419-422 (2014).
- 719 44. Yakir, E. *et al.* Cell autonomous and cell-type specific circadian rhythms in  
720 Arabidopsis. *Plant J.* **68** 520-531 (2011).
- 721 45. Gould, P.D. *et al.* Coordination of robust single cell rhythms in the Arabidopsis  
722 circadian clock via spatial waves of gene expression. *Elife* **7**, e31700 (2018).
- 723 46. Fukuda, H., Ukai, K. & Oyama, T. Self-arrangement of cellular circadian rhythms  
724 through phase-resetting in plant roots. *Phys. Rev. E.* **86**, 041917 (2012).
- 725 47. Takahashi, N., Hirata, Y., Aihara, K. & Mas, P. A hierarchical multi-oscillator network  
726 orchestrates the Arabidopsis circadian system. *Cell* **163**, 148-159 (2015).
- 727 48. James, A.B. *et al.* The circadian clock in Arabidopsis roots is a simplified slave version  
728 of the clock in shoots. *Science* **322**, 1832-1835 (2008).
- 729 49. Nimmo, H.G. Entrainment of Arabidopsis roots to the light:dark cycle by light piping.  
730 *Plant Cell Environ.* **41**, 1742-1748 (2018).
- 731 50. de Montaigu, A., Tóth, R. & Coupland, G. Plant development goes like clockwork.  
732 *Trends in Genetics* **26**, 296-306 (2010).
- 733 51. Kolmos, E. *et al.* A Reduced-Function Allele Reveals That EARLY FLOWERING3  
734 Repressive Action on the Circadian Clock Is Modulated by Phytochrome Signals in  
735 Arabidopsis. *The Plant Cell* (2011).
- 736 52. Dixon, L.E. *et al.* Temporal Repression of Core Circadian Genes Is Mediated through  
737 EARLY FLOWERING 3 in Arabidopsis. *Curr. Biol.* **21**, 120-125 (2011).
- 738 53. Kikis, E., Khanna, R. & Quail, P. ELF4 is a phytochrome-regulated component of a  
739 negative feedback loop involving the central oscillator components CCA1 and LHY.  
740 *Plant Journal* **44**, 300-313 (2005).
- 741 54. Lu, S.X. *et al.* CCA1 and ELF3 Interact in the Control of Hypocotyl Length and  
742 Flowering Time in Arabidopsis. **158**, 1079-1088 (2012).
- 743 55. Huang, H. & Nusinow, D.A. Into the Evening: Complex Interactions in the Arabidopsis  
744 Circadian Clock. *Trends in Genetics* **32**, 674-686 (2016).

- 745 56. Corbesier, L. *et al.* FT Protein Movement Contributes to Long-Distance Signaling in  
746 Floral Induction of Arabidopsis. **316**, 1030-1033 (2007).
- 747 57. Jaeger, K.E. & Wigge, P.A. FT Protein Acts as a Long-Range Signal in Arabidopsis.  
748 *Current Biology* **17**, 1050-1054 (2007).
- 749 58. Mathieu, J., Warthmann, N., Küttner, F. & Schmid, M. Export of FT Protein from  
750 Phloem Companion Cells Is Sufficient for Floral Induction in Arabidopsis. *Current*  
751 *Biology* **17**, 1055-1060 (2007).
- 752 59. Chen, X. *et al.* Shoot-to-Root Mobile Transcription Factor HY5 Coordinates Plant  
753 Carbon and Nitrogen Acquisition. *Current Biology* **26**, 640-646 (2016).
- 754 60. Flis, A. *et al.* Defining the robust behaviour of the plant clock gene circuit with absolute  
755 RNA timeseries and open infrastructure. *Open Biol* **5** (2015).
- 756 61. Salomé, P.A. & McClung, C.R. PSEUDO-RESPONSE REGULATOR 7 and 9 are  
757 partially redundant genes essential for the temperature responsiveness of the  
758 *Arabidopsis* circadian clock. *Plant Cell* **17**, 791-803 (2005).
- 759 62. Edwards, K.D. *et al.* Quantitative analysis of regulatory flexibility under changing  
760 environmental conditions. *Mol. Syst. Biol.* **6** (2010).
- 761 63. Nakagawa, T. *et al.* Development of series of gateway binary vectors, pGWBs, for  
762 realizing efficient construction of fusion genes for plant transformation. *J. Biosci.*  
763 *Bioeng* **104**, 34-41 (2007).
- 764 64. Nakagawa, T. *et al.* Improved gateway binary vectors: high-performance vectors for  
765 creation of fusion constructs in transgenic analysis of plants. *Biosci Biotechnol*  
766 *Biochem.* **71**, 2095-2100 (2007).
- 767 65. Clough, S.J. & Bent, A.F. Floral dip: a simplified method for Agrobacterium-mediated  
768 transformation of *Arabidopsis thaliana*. *Plant J.* **16**, 735-743 (1998).
- 769 66. Plautz, J.D. *et al.* Quantitative analysis of *Drosophila* period gene transcription in living  
770 animals. *J. Biol. Rhythms* **12**, 204-217 (1997).
- 771 67. Czechowski, T., Stitt, M., Altmann, T., Udvardi, M.K. & Scheible, W.-R. Genome-  
772 Wide Identification and Testing of Superior Reference Genes for Transcript  
773 Normalization in Arabidopsis. *Plant Physiology* **139**, 5-17 (2005).
- 774 68. Dobin, A. *et al.* STAR: ultrafast universal RNA-seq aligner. *Bioinformatics* **29**, 15-21  
775 (2013).
- 776 69. Liao, Y., Smyth, G.K. & Shi, W. featureCounts: an efficient general purpose program  
777 for assigning sequence reads to genomic features. *Bioinformatics* **30**, 923-930 (2014).
- 778 70. Robinson, M.D., McCarthy, D.J. & Smyth, G.K. edgeR: a Bioconductor package for  
779 differential expression analysis of digital gene expression data. *Bioinformatics* **26**, 139-  
780 140 (2010).
- 781 71. Love, M.I., Huber, W. & Anders, S.J.G.B. Moderated estimation of fold change and  
782 dispersion for RNA-seq data with DESeq2. *Genome Biol.* **15**, 550 (2014).
- 783 72. Tarazona, S., García-Alcalde, F., Dopazo, J., Ferrer, A. & Conesa, A. Differential  
784 expression in RNA-seq: A matter of depth. *Genome Res.* **21**, 2213-2223 (2011).
- 785 73. Leng, N. *et al.* EBSeq: an empirical Bayes hierarchical model for inference in RNA-seq  
786 experiments. *Bioinformatics* **29**, 1035-1043 (2013).
- 787 74. Robinson, J.T. *et al.* Integrative genomics viewer. *Nat. Biotech.* **29**, 24-26 (2011).
- 788 75. Thorvaldsdóttir, H., Robinson, J.T. & Mesirov, J.P. Integrative Genomics Viewer  
789 (IGV): high-performance genomics data visualization and exploration. *Brief. Bioinform.*  
790 **14**, 178-192 (2013).
- 791 76. Michael, T.P. *et al.* Network discovery pipeline elucidates conserved time-of-day-  
792 specific cis-regulatory modules. *PLoS Genetics* **4**, e14 (2008).
- 793 77. Mockler, T. *et al.* The DIURNAL project: DIURNAL and circadian expression  
794 profiling, model-based pattern matching, and promoter analysis. *Cold Spring Harb.*  
795 *Symp. Quant. Biol.* **72**, 353-363 (2007).
- 796 78. Katari, M.S. *et al.* VirtualPlant: A software platform to support systems biology  
797 research. *Plant Physiol.* **152**, 500-515 (2010).
- 798 79. Takens, F. Detecting strange attractors in turbulence. *Lecture Notes in Math* **898**, 366-  
799 381 (1981).

- 800 80. Stark, J. Delay embeddings for forced systems I. Deterministic forcing. *J. Nonlinear*  
801 *Sci.* **9**, 255-332 (1999).
- 802 81. Marwan, N., Romano, C.M., Thiel, M. & Kurths, J. Recurrence plots for the analysis of  
803 complex systems. *Phys. Rep.* **438**, 237-329 (2007).
- 804 82. Hirata, Y., Horai, S. & Aihara, K. Reproduction of distance matrices and original time  
805 series from recurrence plots and their applications. *Eur. Phys. J. Spec. Top.* **164**, 13-22  
806 (2008).
- 807 83. Tanio, M., Hirata, Y. & Suzuki, H. Reconstruction of driving forces through recurrence  
808 plots. *Phys. Lett. A* **373**, 2031-2040 (2009).
- 809 84. Hirata, Y., Komuro, M., Horai, S. & Aihara, K. Faithfulness of Recurrence Plots: A  
810 Mathematical Proof. *International Journal of Bifurcation and Chaos* **25**, 1550168  
811 (2015).
- 812 85. Khor, A. & Small, M. Examining k-nearest neighbour networks: Superfamily  
813 phenomena and inversion. *Chaos (Woodbury, N.Y.)* **26**, 043101-043101 (2016).
- 814 86. Small, M. *Applied Nonlinear Time Series Analysis: Applications in Physics, Physiology*  
815 *and Finance*. (World Scientific, 2005).

816

## 817 **Acknowledgments**

818 We thank members of the Mas laboratory for helpful discussion and suggestions. We also thank  
819 Prof. T. Nakagawa (Shimane University) and Meiji Seika Kaisha, Ltd. for the Gateway vectors.  
820 We thank J. E. Salazar-Henao for tips on the Western-blot protocol in roots and Dr. I. Rubio-  
821 Somoza for sharing the GFP antibody. Research in Y.H. laboratory is supported by JSPS  
822 KAKENHI (Grant Number JP18K11461). S.J.D laboratory is funded by the Biotechnology and  
823 Biological Sciences Research Council (BB/N018540/1). S.A.K. acknowledges support from the  
824 National Institute of Health (GM067837). The Mas laboratory is funded from the  
825 FEDER/Spanish Ministry of Economy and Competitiveness, from the Ramon Areces  
826 Foundation and from the Generalitat de Catalunya (AGAUR). P.M. laboratory also  
827 acknowledges financial support from the CERCA Program/Generalitat de Catalunya and by the  
828 Spanish Ministry of Economy and Competitiveness through the “Severo Ochoa Program for  
829 Centers of Excellence in R&D” 2016–2019 (SEV-2015-0533). W.W.C. is a recipient of a CSC  
830 (Chinese Scholarship Council) fellowship.

## 831 **Author Contributions**

832 W.W.C, N.T. and J.R. performed the biological experiments. Y.H. performed the mathematical  
833 analysis. S.P., S.J.D., D.A.N. and S.A.K. contributed with reagents and comments. P.M.  
834 designed the experiments and wrote the manuscript. All authors read, revised, and approved the  
835 manuscript.

## 836 **Competing interests**

837 The authors declare no competing interests.

## 838 **Additional information**

839 Extended data is available for this paper at XXX.

840 Supplementary information is available for this paper at XXX.

## 841 Figure Legends

842

843 **Fig. 1. Prevalent function of ELF4 sustaining circadian rhythms in roots.** **a**, Luminescence  
844 of *CCA1::LUC* (*LUCIFERASE*) oscillation simultaneously measured in shoots (Sh)  
845 (n=9) and roots (Rt) (n=9). Root luminescence signals are represented in the right Y-axis. **b**,  
846 Period (left Y-axis) estimates of *CCA1::LUC* rhythms in shoots and roots (n=8 for each)  
847 and amplitude (right Y-axis) estimates of *CCA1::LUC* rhythms in shoots (n=7) and  
848 roots (n=8); data are represented as the median  $\pm$  max and min; 25-75 percentile). \*\*\* p-  
849 value<0.0001; two-tailed t-tests with 95% of confidence. **c**, Circadian time course  
850 analyses of *CCA1* mRNA expression in WT Sh and Rt. **d**, Luminescence of  
851 *CCA1::LUC* rhythms in WT (n=9) and *elf4-1* Rt (n=8). **e**, Luminescence of *LHY::LUC*  
852 rhythms in WT (n=8) and ELF4-ox Rt (n=9). **f**, Circadian time course analyses of *PRR9*  
853 mRNA expression in roots of WT and *elf4-1*. Sampling was performed under constant  
854 light conditions (LL) following synchronization under light:dark cycles (LD). **a**, **c-f**,  
855 Data are represented as the means + SEM. **g**, Heatmap of the median-normalized expression (Z-  
856 scaled FPKM values) of DEGs following a hierarchical clustering using the Euclidean  
857 distance. **h**, Relationship between average expression and fold change for each gene. **i**,  
858 Volcano plot showing fold-change versus significance of the differential expression test.  
859 Black dots represent genes that are not differentially expressed, while red and green dots  
860 are the genes that are significantly up- and down-regulated, respectively. Circadian  
861 phases of **j**, up- and **k**, down-regulated DEG in *elf4-1* roots. Radial axis represents the  
862 subjective time (hours). White and gray areas represent subjective day and night,  
863 respectively. The “n” values refer to independent samples. **a-k**, Data for all experiments  
864 are representative of two biological replicates, with measurements taken from distinct  
865 samples grown and processed at different times.

866

867 **Fig. 2. ELF4 moves from shoots to regulate rhythms in roots.** *CCA1::LUC* luminescence in  
868 roots of ELF4-ox scion into **a**, *elf4-1* (n=4) and **b**, *elf4-2* (n=3) rootstocks. Water instead of  
869 luciferin was added to the wells containing ELF4-ox shoots. *CCA1::LUC* luminescence in *elf4-1*  
870 rootstocks with **c**, WT (n=8) and **d**, ELF4 Minigene (ELF4MG) (n=10) scions. WT scions do  
871 not express reporters and water instead of luciferin was added to the wells containing ELF4MG  
872 shoots. **a-d**, Schematic drawings depicting the different scion/rootstock combinations are shown  
873 above each graph. **e**, Circadian time course analyses of *ELF4* mRNA expression in roots of WT,  
874 *elf4-1* and ELF4-ox scion and *elf4-1* rootstocks. **f**, Luminescence of *LHY::LUC* rhythms in *elf4-*



875 *l* roots after injection in shoots of purified ELF4 (n=4) or GFP proteins (n=8) and *elf4-1* roots  
876 as a control (n=6). **g**, Representative image showing the lack of fluorescence signals in roots of  
877 WT scion and WT rootstock. **h**, Representative image showing fluorescence signals in roots of  
878 ELF4-ox scion into *elf4-1* rootstock. Scale bar: 100  $\mu$ m. **i**, Western-blot analysis of ELF4-GFP  
879 protein accumulation (arrows) in roots of ELF4-ox-GFP scion (E4ox) grafted into *elf4-1*  
880 rootstock (*e4-1*) (two pools of independent grafting assays, #1 and #2, are shown). Asterisks  
881 denote non-specific bands. **j**, *CCA1::LUC* luminescence in *elf4-2* rootstocks grafted with  
882 ELF4-x3GFP scions (n=5). Water instead of luciferin was added to the wells containing ELF4-  
883 x3GFP shoots. **a-f, j**, Data are represented as the means + SEM. **k**, Protein features of various  
884 plant mobile proteins. The “n” values refer to independent samples. **a-j**, Two biological  
885 replicates were performed for all experiments, with measurements taken from distinct samples  
886 grown and processed at different times.

887  
888 **Fig. 3. Mobile ELF4 does not regulate the photoperiodic-dependent phase in roots.**

889 Luminescence analyses of *PRR9::LUC* rhythms in **a**, roots (n=5 for ShD, n=6 for LgD) and **b**,  
890 shoots (n=6 for ShD, n=4 for LgD) of plants grown under short day (ShD) or long day (LgD)  
891 conditions. **c**, Western-blot analyses and **d**, quantification of ELF4 protein accumulation in  
892 ELF4 Minigene roots (E4MG Rt) of plants grown under ShD and LgD (also in Extended Data  
893 Fig. 8a-d). **e**, Western-blot analyses and **f**, quantification of ELF4 protein accumulation in  
894 E4MG roots of plants grown under ShD and excised roots under LgD (also in Extended Data  
895 Fig. 8a-f). Arrows indicate the ELF4 protein. Luminescence of *LHY::LUC* oscillation in WT,  
896 ELF4-ox and *elf4-1* plants measured in **g**, shoots (Sh) (n=12) and **h**, roots (Rt) (n=12) under  
897 LgD conditions. **a-b, d, f, g-h**, Data are represented as the means + SEM. Dashed lines indicate  
898 dusk under LgD. The “n” values refer to independent samples. **a-h**, Two biological replicates  
899 were performed for all experiments, with measurements taken from distinct samples grown and  
900 processed at different times.

901  
902 **Fig. 4. Mobile ELF4 sets the temperature-dependent pace of the root clock.**

903 Individual luminescence waveforms of *CCA1::LUC* rhythmic oscillation in ELF4-ox scion into  
904 *elf4-1* rootstocks at **a**, 12°C (n=10) and **b**, 28°C (n=8). Individual luminescence waveforms of  
905 *CCA1::LUC* rhythmic oscillation in E4MG scion into *elf4-1* rootstocks at **c**, 12°C (n=7) and **d**,  
906 28°C (n=8). Water instead of luciferin was added to the wells containing ELF4-ox and E4MG  
907 scions. **e**, Luminescence of *LHY::LUC* rhythmic oscillation in WT and ELF4-ox roots at 28°C  
908 (n=8 for WT, n=5 for ELF4-ox). Data are represented as the means + SEM. **f**, Western-blot  
909 analysis of ELF4-GFP protein accumulation (arrow) in roots of ELF4-ox-GFP scion (E4ox)  
910 grafted into *elf4-1* rootstock (*e4-1*) at 12°C and 28°C. *elf4-1* mutant protein extracts were used

911 as a control. Asterisks denote non-specific bands. Ponceau S staining of the membrane is shown  
912 in the right panel. Schematic drawing depicting **g**, the increased shoot-to-root movement of  
913 ELF4 (Sh-to-Rt mov, thick blue vertical arrows), increased *PRR9* repression and the slow pace  
914 of the root clock at low temperatures, and **h**, the decreased shoot-to-root movement (Sh-to-Rt  
915 mov, thin red vertical arrows), decreased *PRR9* repression and fast-paced root clock at high  
916 temperature. The “n” values refer to independent samples. **a-f**, Two biological replicates were  
917 performed for all experiments, with measurements taken from distinct samples grown and  
918 processed at different times.

Figure 1

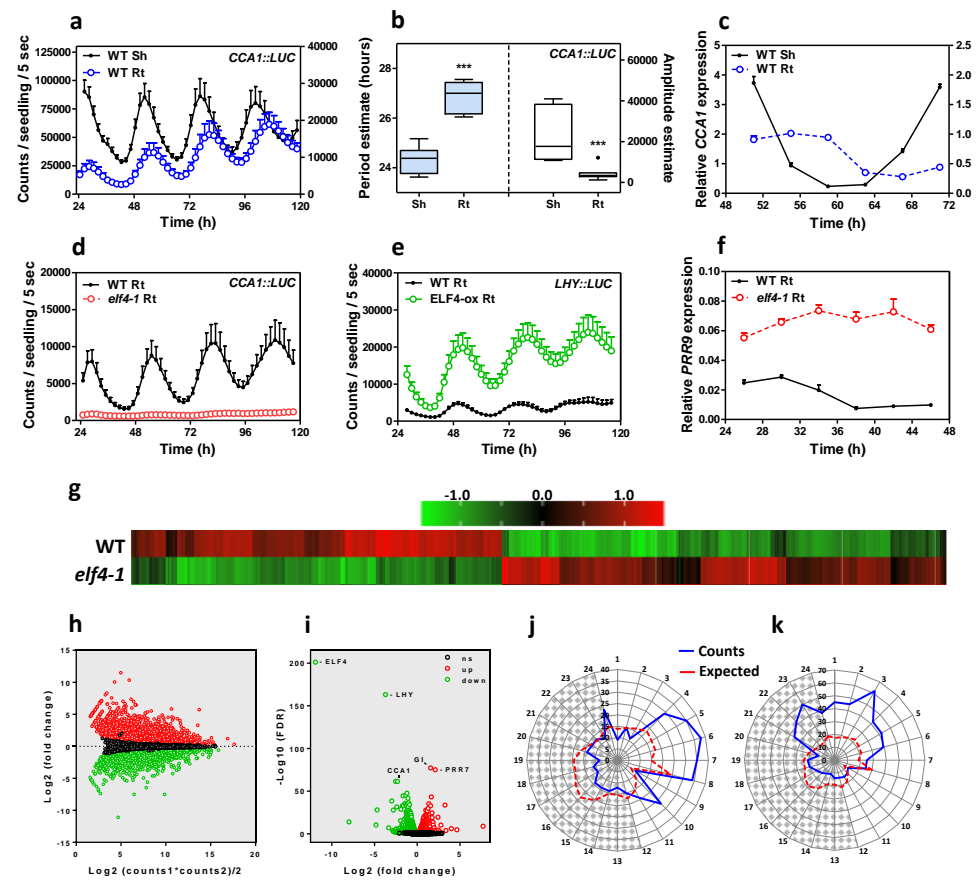


Figure 2

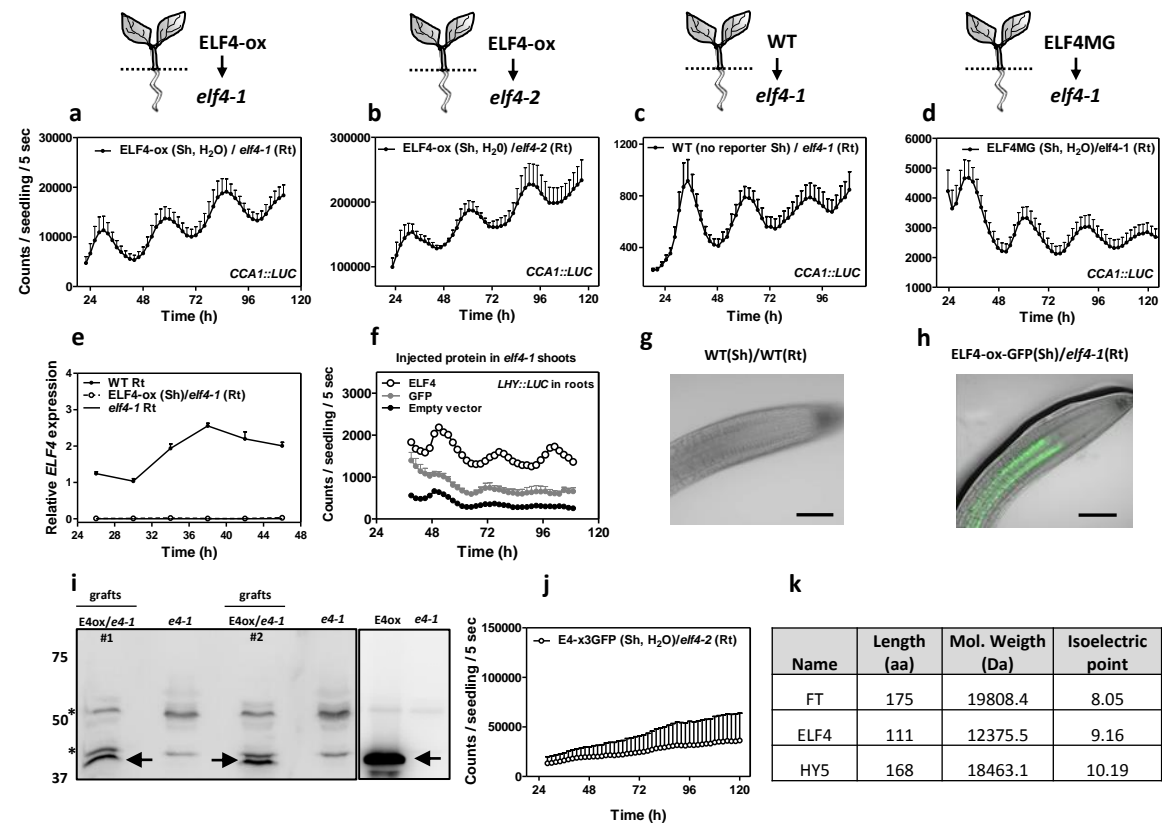


Figure 3

